International Journal of Fracture **43**: 1–18, 1990.

Interface crack between two elastic layers

ZHIGANG SUO and JOHN W. HUTCHINSON
Division of Applied Sciences, Harvard University, Cambridge, Massachusetts 02138, USA

Received 20 April 1988; accepted 10 October 1988

Abstract. A semi-infinite interface crack between two infinite isotropic elastic layers under general edge loading conditions is considered. The problem can be solved analytically except for a single real scalar independent of loading, which is then extracted from the numerical solution for one particular loading combination. Two applications of the basic solution are made which illustrate its utility: interface cracking driven by residual stress in a thin film on a substrate, and an analysis of a test specimen proposed recently for measuring interface toughness.

1. Introduction

Thin films are susceptible to decohesion from substrates due to their elastic and/or thermal mismatch. When load (either mechanical or thermal) is applied to the film, cracks may initiate and propagate along the interface or in the substrate approximately paralleling the interface [1–4]. The latter case has been considered in [2, 3] and will be further studied elsewhere by the present authors [4] using methods similar to those developed here. The aim of this paper is to analyze interface cracks between thin films and substrates under fairly general loading conditions. The solution can be readily applied to a wide range of problems, two of which are given here.

The mathematical problem which is analyzed is introduced in Fig. 1a. Each material is taken to be isotropic and linearly elastic with material #1 lying above the interface which coincides with the x_1-axis and #2 below. The thickness of the two layers are h and H, respectively. A semi-infinite crack lies along the negative x_1-axis with the tip at the origin. The uncracked bimaterial layer can be regarded as a composite beam with a neutral axis lying a distance δ above the bottom of layer #2. The expression for δ is given in Appendix III. The structure is loaded as is shown in Fig. 1a, where the P's are loads per unit thickness and the M's are moments per unit thickness. Overall equilibrium provides two constraints among the six load parameters. That is

$$\begin{aligned} &P_1 - P_2 - P_3 = 0, \\ &M_1 - M_2 + P_1\left(\frac{h}{2} + H - \delta\right) + P_2\left(\delta - \frac{H}{2}\right) - M_3 = 0. \end{aligned} \tag{1.1}$$

Hence only four among the six are independent, say, P_1, P_3, M_1, and M_3.

Since $\sigma_{22} = \sigma_{12} = 0$ in the layers in Fig. 1b, a crack can be created anywhere paralleling the interface without disturbing stress distribution. The singular fields for the problem in Fig. 1a are therefore exactly the same as those for the problem in Fig. 1c when the problem

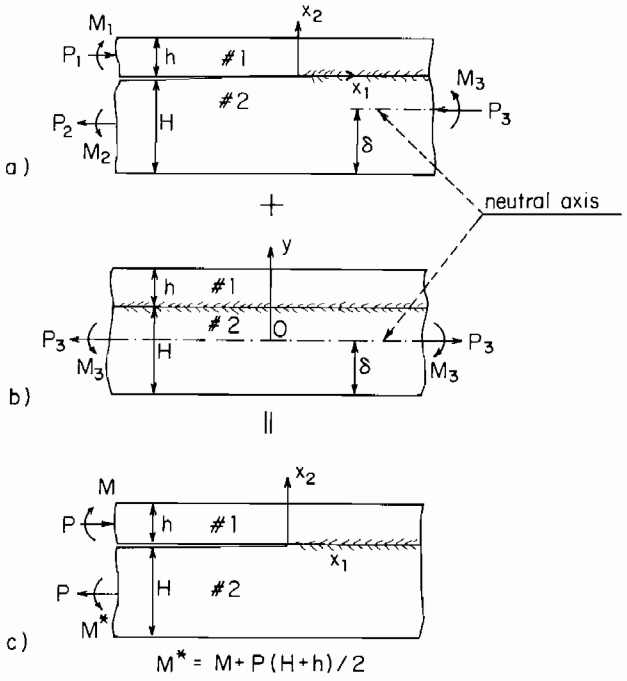

Fig. 1. Conventions and geometry.

in Fig. 1b is superimposed. This superposition shows that the number of load parameters controlling the crack tip singularity can be reduced to only two, P and M, given by

$$P = P_1 - C_1 P_3 - C_2 \frac{M_3}{h},$$
$$M = M_1 - C_3 M_3. \tag{1.2}$$

The C's are dimensionless numbers defined in Appendix III. It is the problem in Fig. 1c that will be analyzed in Section 2. Once the solution to the problem in Fig. 1c is obtained, the solution to the problem in Fig. 1a can be readily constructed by reinterpreting P and M by (1.2).

The general nature of the edge loads of the system in Fig. 1a makes it possible to solve some special problems of practical interest. Two sample problems are considered in Section 3 for the purpose of illustration. The first is concerned with residually stressed thin films. Figures 2a–d show that, by the "cut and paste" technique, the stress intensity induced by residual stress can be simulated by a special combination of edge loads. The second sample problem is the four-point bending test specimen (Fig. 3a) recently proposed by Charalambides et al. [5] for determining the fracture toughness of bimaterial interfaces. It has been slightly extended here to include an independently applied longitudinal load in order to assess whether it is feasible to use such a specimen to measure toughness over the full range of mixed-mode interface intensity factors. When the crack is long compared to the thickness of the top layer but still lying within the central region of the specimen, the specimen can be well approximated by the system in Fig. 3b. The latter is simply a special loading case of the system in Fig. 1a.

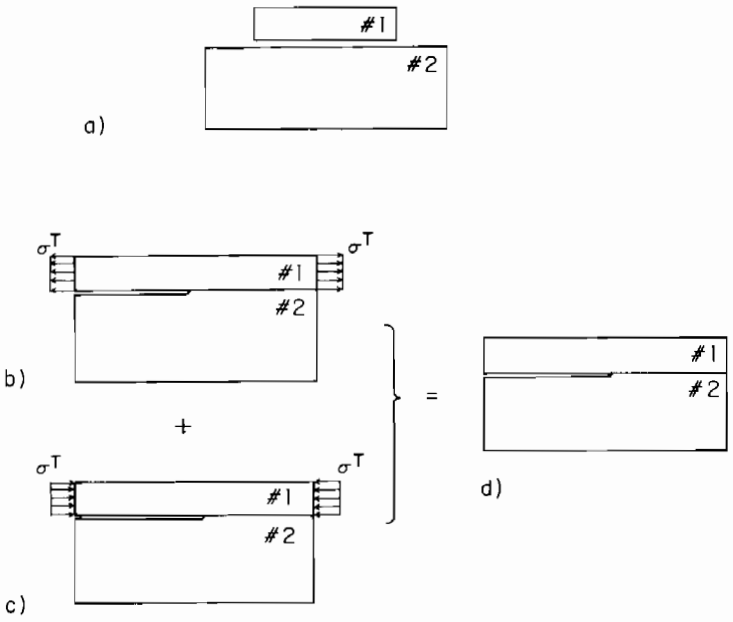

Fig. 2. Cut and paste procedure for constructing solution to interface crack driven by residual stress.

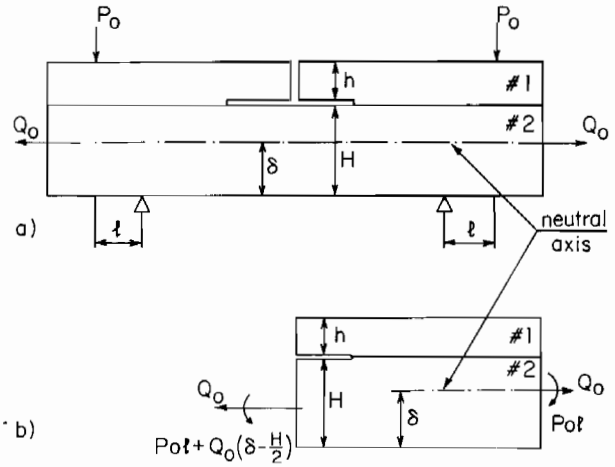

Fig. 3. (a) Four-point bend specimen with longitudinal load. (b) Equivalent edge loading.

2. Energy release-rate and stress intensity factors

As observed by Dundurs [7] the elastic moduli dependence of a bimaterial system, with some restrictions, may be expressed in terms of two (rather than three) special non-dimensional combinations. The Dundurs' parameters adopted in this paper are defined as

$$\alpha = \frac{\Gamma(\kappa_2 + 1) - (\kappa_1 + 1)}{\Gamma(\kappa_2 + 1) + (\kappa_1 + 1)},$$
$$\beta = \frac{\Gamma(\kappa_2 - 1) - (\kappa_1 - 1)}{\Gamma(\kappa_2 + 1) + (\kappa_1 + 1)}. \tag{2.1}$$

Subscripts 1 and 2 refer to the two materials in Fig. 1, $\kappa = 3\text{–}4\nu$ for plane strain and $(3 - \nu)/(1 + \nu)$ for plane stress, $\Gamma = \mu_1/\mu_2$, ν is Poisson's ratio, and μ shear modulus. The physically admissible values of α and β are restricted to a parallelogram enclosed by $\alpha = \pm 1$ and $\alpha - 4\beta = \pm 1$ in the α, β-plane, assuming the Poisson ratios do not take on negative values. This will be of advantage later on when the discussion of functions that depend on material combinations is made.

The linear elasticity singularity solution in the crack tip region can be developed using the bimaterial constant ε, defined as

$$\varepsilon = \frac{1}{2\pi} \ln \frac{1 - \beta}{1 + \beta}. \tag{2.2}$$

The complex stress intensity factor $K \equiv K_1 + iK_2$ has been introduced, following Rice [6] and Hutchinson et al. [8], such that the traction a distance r ahead of the crack tip is given by

$$\sigma_{22} + i\sigma_{12} = \frac{K}{\sqrt{2\pi r}} r^{i\varepsilon} \tag{2.3}$$

where $i = \sqrt{-1}$, and the crack face displacements a distance r behind the crack tip are given by

$$\delta_2 + i\delta_1 = \frac{c_1 + c_2}{2\sqrt{2\pi}(1 + 2i\varepsilon) \cosh(\pi\varepsilon)} K\sqrt{r} r^{i\varepsilon}, \tag{2.4}$$

where the compliance parameters are

$$c_1 = \frac{\kappa_1 + 1}{\mu_1}, \quad c_2 = \frac{\kappa_2 + 1}{\mu_2}. \tag{2.5}$$

The energy release per unit of new crack area, in terms of the complex stress intensity factor K, is

$$\mathcal{G} = \frac{c_1 + c_2}{16 \cosh^2 \pi\varepsilon} |K|^2. \tag{2.6}$$

The analysis of the system in Fig. 1c is now taken up. The energy release rate can be computed exactly within the context of plane stress or plane strain by taking the difference between the energy stored in the structure per unit length far ahead and far behind the crack tip. Calculations for similar problems based on the J-integral can be found in [9]. The result is a positive definite quadratic in P and M which can be written as

$$\mathcal{G} = \frac{c_1}{16}\left[\frac{P^2}{Ah} + \frac{M^2}{Ih^3} + 2\frac{PM}{\sqrt{AI}h^2} \sin\gamma\right], \tag{2.7}$$

where A and I are positive dimensionless numbers and the angle γ is restricted such that $|\gamma| \leqslant \pi/2$ for definiteness. These quantities are given by

$$A = \frac{1}{1 + \Sigma(4\eta + 6\eta^2 + 3\eta^3)}, \quad I = \frac{1}{12(1 + \Sigma\eta^3)},$$
$$\sin\gamma = 6\Sigma\eta^2(1 + \eta)\sqrt{AI}, \quad \Sigma = \frac{c_2}{c_1} = \frac{1 + \alpha}{1 - \alpha}, \quad \eta = \frac{h}{H}. \tag{2.8}$$

Without loss of generality, attention will be restricted to $h \leqslant H$ or equivalently, $0 \leqslant \eta \leqslant 1$.

The magnitude of the complex stress intensity factor can be obtained readily by comparing (2.6) and (2.7). That is

$$|K|^2 = \frac{p^2}{2}\left[\frac{P^2}{Ah} + \frac{M^2}{Ih^3} + 2\frac{PM}{\sqrt{AI}h^2}\sin\gamma\right], \tag{2.9}$$

where

$$p = \sqrt{\frac{1 - \alpha}{1 - \beta^2}}. \tag{2.10}$$

It is interesting to note that $|K|$ depends on β only through p.

Arguments similar to those in [1] and [8] are exploited to determine the real and imaginary parts of the complex stress intensity factor. From dimensional considerations and by linearity it follows that the complex stress intensity factor K can be written in the form

$$K = \left(a\frac{P}{\sqrt{Ah}} + b\frac{M}{\sqrt{Ih^3}}\right)\frac{p}{\sqrt{2}}h^{-i\varepsilon}, \tag{2.11}$$

where a and b are dimensionless complex numbers which only depend on the geometric parameter η and Dundurs' parameters α and β, but not on P, M or h. Substitution of (2.11) into (2.9) yields

$$|a| = 1, \quad |b| = 1, \quad \bar{a}b + a\bar{b} = 2\sin\gamma. \tag{2.12}$$

The only physically meaningful solution to (2.12) can be written as

$$a = e^{i\omega}, \quad b = -ie^{i(\omega+\gamma)}, \tag{2.13}$$

where the real angular quantity ω only depends on η, α and β, and can be chosen in the range $0 \leqslant \omega \leqslant \pi/2$. Thus it is possible to rewrite (2.11) as

$$K \equiv K_1 + iK_2 = \left(\frac{P}{\sqrt{Ah}} - ie^{i\gamma}\frac{M}{\sqrt{Ih^3}}\right)\frac{p}{\sqrt{2}}h^{-i\varepsilon}e^{i\omega}, \tag{2.14}$$

so that the stress intensity factor is fully determined apart from the single dimensionless real scalar function $\omega(\alpha, \beta, \eta)$.

As suggested in [5, 6, 8], it is sometimes convenient to consider the combination $Kh^{i\varepsilon}$ in the complex plane according to

$$Kh^{i\varepsilon} = |K|e^{i\psi}, \tag{2.15}$$

since $|Kh^{i\varepsilon}| = |K|$. By (2.14),

$$\begin{aligned} \text{Re}\,[Kh^{i\varepsilon}] &= \frac{p}{\sqrt{2}}\left[\frac{P}{\sqrt{Ah}}\cos\omega + \frac{M}{\sqrt{Ih^3}}\sin(\omega+\gamma)\right], \\ \text{Im}\,[Kh^{i\varepsilon}] &= \frac{p}{\sqrt{2}}\left[\frac{P}{\sqrt{Ah}}\sin\omega - \frac{M}{\sqrt{Ih^3}}\cos(\omega+\gamma)\right]. \end{aligned} \tag{2.16}$$

The phase angle ψ defined in (2.15) is given by

$$\psi = \tan^{-1}\left[\frac{\lambda\sin\omega - \cos(\omega+\gamma)}{\lambda\cos\omega + \sin(\omega+\gamma)}\right], \tag{2.17}$$

where λ measures the loading combination as

$$\lambda = \sqrt{\frac{I}{A}}\frac{Ph}{M}. \tag{2.18}$$

Specific determination of the function $\omega(\alpha, \beta, \eta)$ requires that the crack problem be rigorously solved for one loading case for given α, β and η. This has been done using integral equation methods; the details of the solution procedure are given in Appendix I. The function $\omega(\alpha, \beta, \eta)$ is summarized in Tables 1–4 for various α and β at $\eta = 0, 0.1, 0.5$ and 1. The dependence of ω on the three variables is relatively weak. Over the whole of the parameters ω only varies between about 37° to 65°. For fixed α and β, ω varies even less as η varies from 0 to 1. Therefore the ω vs. η relation for fixed α and β can be well approximated by linear interpolation between any two stations of η where values of ω are presented in Tables 1–4.

Table 1. $\omega(\alpha, \beta, 0)$ (in degrees)

β \ α	−0.8	−0.6	−0.4	−0.2	0.0	0.2	0.4	0.6	0.8
−0.4	64.4	66.0							
−0.3	60.2	61.3	62.5	63.9					
−0.2	55.5	56.6	57.9	59.3	60.8	62.9			
−0.1	51.0	52.1	53.4	54.9	56.5	58.4	60.9	64.9	
0.0	46.7	47.8	49.0	50.4	52.1	54.1	56.7	60.1	65.7
0.1			44.6	46.1	47.8	49.8	52.5	56.1	62.0
0.2					43.4	45.5	48.2	52.1	57.0
0.3							44.0	47.8	54.9
0.4									50.3

Table 2. $\omega(\alpha, \beta, 0.1)$ (in degrees)

β \ α	−0.8	−0.6	−0.4	−0.2	0.0	0.2	0.4	0.6	0.8
−0.4	64.5	65.2							
−0.3	59.9	60.5	61.5	64.0					
−0.2	55.2	56.0	56.9	58.1	61.5	63.6			
−0.1	50.6	51.5	52.5	55.4	57.1	59.1	61.3	64.4	
0.0	46.0	49.0	50.9	52.7	54.6	56.5	58.9	62.0	64.0
0.1			43.4	44.7	42.3	50.4	53.2	56.5	60.9
0.2					44.0	46.4	49.1	52.4	57.7
0.3							44.7	48.4	53.9
0.4									49.9

Table 3. $\omega(\alpha, \beta, 0.5)$ (in degrees)

β \ α	−0.8	−0.6	−0.4	−0.2	0.0	0.2	0.4	0.6	0.8
−0.4	64.1	64.5							
−0.3	59.3	59.8	60.6	61.6					
−0.2	53.3	55.2	56.1	57.1	58.4	59.9			
−0.1	50.0	50.8	51.5	52.8	54.1	55.6	57.5	59.7	
0.0	45.3	46.1	47.2	48.4	49.8	51.4	54.6	56.8	59.2
0.1			43.0	43.9	45.6	47.3	49.4	51.8	55.2
0.2					41.2	43.0	45.1	47.8	51.4
0.3							40.7	43.6	47.4
0.4									43.2

Table 4. $\omega(\alpha, \beta, 1)$ (in degrees)

β \ α	−0.8	−0.6	−0.4	−0.2	0.0	0.2	0.4	0.6	0.8
−0.4	63.7	64.6							
−0.3	58.5	59.5	60.8	62.1					
−0.2	53.7	54.5	55.8	57.2	58.7	60.3			
−0.1	48.9	49.7	51.0	52.3	53.8	55.4	57.2	59.6	
0.0	44.2	44.9	46.2	47.6	49.1	50.8	52.6	55.0	57.2
0.1			41.6	42.9	44.4	46.0	47.8	49.8	52.4
0.2					39.5	41.2	43.0	45.1	47.6
0.3							38.0	40.1	42.8
0.4									37.6

The present solution can be related to two special cases whose solutions are known, in each case for the limit of a homogeneous material ($\alpha = \beta = 0$). When $\alpha = \beta = 0$, the interface intensity factors K_1 and K_2 reduce to the classical mode I and mode II factors, K_I and K_{II}. The case in which $\eta = 1$ can be solved immediately and exactly by noting that symmetry requires $K_2 = 0$ when $P = 0$. Specializing (2.16) to this case, noting $\sin \gamma = \sqrt{(3/7)}$, and enforcing $K_2 = 0$ for $P = 0$, one finds $\omega = \pi/2 - \gamma = \cos^{-1}[\sqrt{(3/7)}] = 49.107°$. Our computed value for this case is 49.110°. The exact result for $\eta = 1$ is

$$K_I = \sqrt{3}Ph^{-1/2} + 2\sqrt{3}Mh^{-3/2}, \quad K_{II} = 2Ph^{-1/2}. \tag{2.19}$$

The second case is the limit $\eta = 0$ given by Thouless et al. [1], also obtained by numerical means. In this case (2.16) reduces to

$$K_{\mathrm{I}} = \frac{1}{\sqrt{2}}[Ph^{-1/2}\cos\omega + 2\sqrt{3}Mh^{-3/2}\sin\omega],$$
$$K_{\mathrm{II}} = \frac{1}{\sqrt{2}}[Ph^{-1/2}\sin\omega - 2\sqrt{3}Mh^{-3/2}\cos\omega], \tag{2.20}$$

and the ω-value extracted from the result in [1] is $\omega = 52.14°$. The present computations give $\omega = 52.08°$ for this case, and we believe that the present result is probably the more accurate of the two. These comparisons and the additional consistency checks discussed in Appendix I suggest the numerical results in the Tables are accurate to within a few tenths of a percent.

3. Sample applications

The two problems mentioned in the Introduction are now considered to illustrate the general applicability of the basic solution developed in the last section. The procedure for each one includes:

(i) reducing the problem to the system in Fig. 1a with special loads,
(ii) calculating the equivalent loads P and M with (1.2), and finally
(iii) substituting P and M into one of the expressions for the interface stress intensity factor, (2.14) or (2.9) and (2.17).

First consider the residually stressed thin film problem introduced in Fig. 2. Here σ^T is the uniform tensile "misfit" stress in the film (the upper layer) relative to the substrate. For example, for two layers of infinite extent in the x_1 and x_3 directions which are unstressed and bonded at temperature T_0 and then cooled to T, $\sigma^T = 8\Delta\alpha(T - T_0)/c_1$, where $\Delta\alpha$ is the coefficient of thermal expansion of material #1 minus that of #2. (Note that σ^T is the misfit stress and *not* the residual stress in the film. Only when $\eta = 0$ are the two the same.) The "cut and paste" technique indicates that, as in Fig. 2c, the stress intensity factor of the interface crack associated with residual stressing due to σ^T is exactly equivalent to that induced by the following load and moment combinations in Fig. 1a:

$$P_1 = P_3 = \sigma^T h, \quad M_3 = \sigma^T h\left(H - \delta + \frac{h}{2}\right), \quad M_1 = 0. \tag{3.1}$$

The equivalent loads are calculated using (1.2), i.e.,

$$P = \sigma^T h\left[1 - C_1 - C_2\left(\frac{1}{\eta} - \Delta + \frac{1}{2}\right)\right], \quad M = -\sigma^T h^2 C_3\left(\frac{1}{\eta} - \Delta + \frac{1}{2}\right), \tag{3.2}$$

where the expression for $\Delta \equiv \delta/h$ is given in Appendix III. These equivalent loads can be used to determine K for arbitrary values of α, β and η. In the limit when the film is very thin

compared to the substrate, $\eta \to 0$, one finds from (2.14)

$$K \equiv K_1 + iK_2 = p\sigma^T \left(\frac{h}{2}\right)^{1/2} h^{-i\varepsilon} e^{i\omega(\alpha,\beta,0)}. \tag{3.3}$$

As suggested in [11], insight into interfacial crack behavior without the complications arising from nonzero ε can be obtained by considering material combinations such that $\alpha \neq 0$ but $\beta = 0$, since by (2.2) ε vanishes when β does. For such material combinations there is no oscillatory behavior and, moreover, K_1 and K_2 measure the tensile and shearing stress singularities, respectively, on the interface ahead of the crack with the standard definition of an intensity factor, as can be seen by (2.3). When $\beta = 0$, (3.3) reduces to

$$K_1 + iK_2 = \sqrt{1 - \alpha}\sigma^T (h/2)^{1/2} e^{i\omega(\alpha,0,0)}. \tag{3.4}$$

The residual stress gives rise to comparable values of K_1 and K_2 (i.e., tension and shear across the interface) since ω always lies between about 45° and 65°. Note that a compressive misfit stress would give rise to a negative value of K_1 according to (3.4). The solution is then inadmissible because the crack would not open and contact between crack faces has not been considered.

The second application is the four-point bend specimen recently proposed by Charalambides et al. [5] for determining the fracture resistance of bimaterial interfaces (see Fig. 2a). At the suggestion of M.F. Ashby (private communication), the role of a load component parallel to the specimen has been considered here to assess whether it is possible to generate all combinations of K_1 and K_2 by varying the relative amounts of the two loads P_0 and Q_0. As is clear from Fig. 3, the stress intensity factors can be computed from the solution to the problem in Fig. 1a if the following identification is made

$$P_1 = M_1 = 0, \quad P_3 = -Q_0, \quad M_3 = -P_0 l. \tag{3.5}$$

Define a magnitude S and phase angle ϕ of the loading combination by

$$Q_0 + iP_0(l/h) = Se^{i\phi}. \tag{3.6}$$

By (1.2) the equivalent loads P and M are

$$P = S(C_1 \cos\phi + C_2 \sin\phi), \quad M = ShC_3 \sin\phi. \tag{3.7}$$

The range of loading is limited to that in which the crack remains open, except for possible contact in the immediate vicinity of the crack tip which always occurs if $\varepsilon \neq 0$. By (2.16), Re $[Kh^{i\varepsilon}] \geqslant 0$ if the loading angle ϕ is restricted to the range

$$-\phi^* \leqslant \phi \leqslant \pi - \phi^*, \tag{3.8}$$

where

$$\tan\phi^* = C_1 \cos\omega[C_2 \cos\omega + (A/I)^{1/2} C_3 \sin(\omega + \gamma)]^{-1}. \tag{3.9}$$

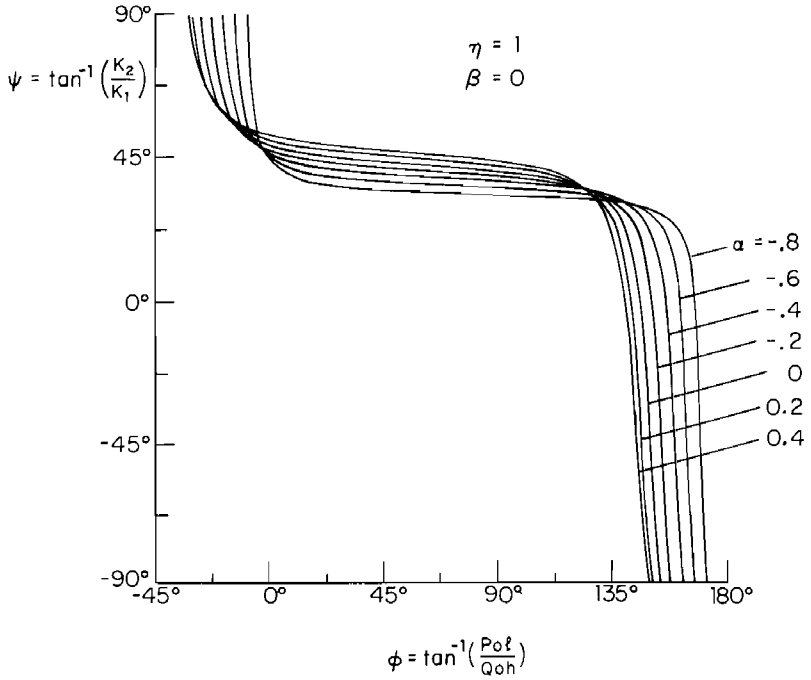

Fig. 4. Relation between combination of K_1 and K_2 at interface crack tip and combination of applied loads on the specimen.

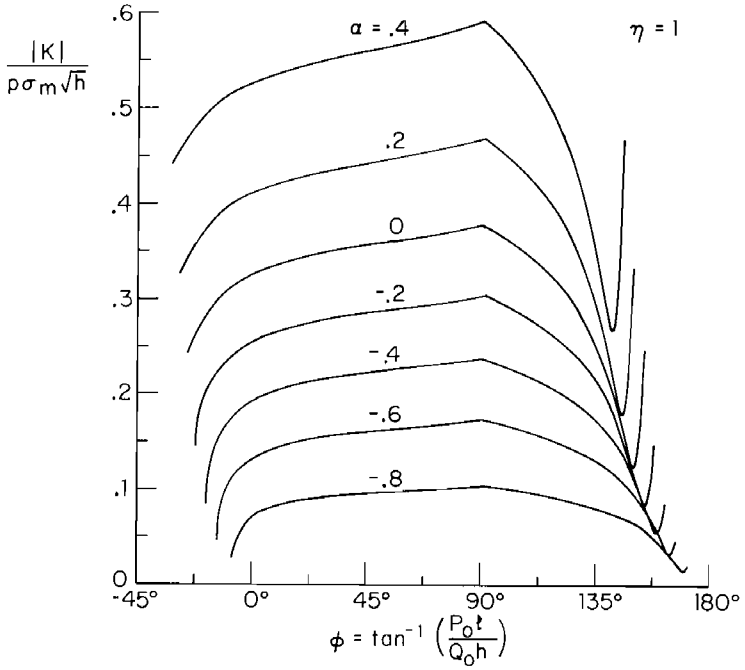

Fig. 5. Normalized magnitude of interface stress intensity factor as a function of the combination of applied loads on the specimen.

The angle ψ characterizing the relative proportion of the stress intensity factors can be calculated in terms of ϕ by substituting (3.7) into (2.17). Curves of ψ versus ϕ are plotted in Fig. 4 for $\eta = 1$ for various α, all with $\beta = 0$. As already noted, when $\beta = 0$, $\psi = \tan^{-1}(K_2/K_1)$ and the condition that the crack is open is simply $K_1 > 0$. For ϕ ranging from about 0° to 90°, ψ varies slowly. Towards the ends of the range of loading combinations ψ varies rapidly with ϕ. The magnitude of the complex stress intensity factor is plotted as a function of ϕ in Fig. 5. In this plot $|K|$ has been normalized by $p\sigma_m\sqrt{h}$ where σ_m is the maximum tensile or compressive stress occurring in the lower layer at the center of the specimen, calculated assuming the crack length is long compared to h. Notice that in Fig. 5 the normalized quantity $|K|/(p\sigma_m\sqrt{h})$ is exact and independent of β. The fact that this normalized $|K|$ remains robust over essentially the entire range of loading combinations suggests that it may be feasible to develop such a specimen. The rapid variation of ψ with ϕ towards the ends of the loading range will probably require highly accurate control of the loads.

4. Concluding remarks

The present study has provided the complete solution to the semi-infinite crack lying along the interface of two infinite elastic layers subjected to general edge loads. The solution is otherwise analytic and exact except for the function $\omega(\alpha, \beta, \eta)$, which has been calculated extensively for the convenience of future application. As indicated by the two practical problems, the basic solution may help interpret some important experimental data in the further study of thin film and interface phenomena.

Acknowledgements

This work was supported in part by DARPA University Research Initiative (Subagreement P.O. #VB38639-0 with the University of California, Santa Barbara, ONR Prime Contract N00014-86-K-0753), by the National Science Foundation under Grant MSM-84-16392, and by the Division of Applied Sciences, Harvard University.

Appendix I

In this Appendix we set up and solve the integral equation for the plane elasticity problem specified in Fig. 1c. A semi-infinite crack lies along the interface of two infinite layers. Each material is taken to be isotropic and linearly elastic with material #1 lying above the x_1-axis and #2 below. The thickness of the two layers are $h = 1$ and $H = 1/\eta$, respectively. The bottom and top surfaces of the bimaterial layer are traction-free. Edge loads are prescribed as

$$P = 1, \quad M = m, \quad M^* = m + (1 + 1/\eta)/2. \tag{AI.1}$$

Let $b_i(\xi)$ be the x_i component of an edge dislocation located on the interface at $x_1 = \xi$. The stresses at $x_1 = x$ on the interface induced by the dislocation are given by

$$\sigma_{22}(x) + i\sigma_{12}(x) = \frac{2\bar{B}(\xi)}{x - \xi} + 2\pi\beta i\delta(x - \xi)\bar{B}(\xi) + B(\xi)F_1(x - \xi) + \bar{B}(\xi)F_2(x - \xi), \tag{AI.2}$$

where $i = \sqrt{-1}$, $\delta(x)$ is the Dirac delta function and

$$B(\xi) = \frac{1 + \alpha}{c_2(1 - \beta^2)} \frac{1}{\pi i} [b_1(\xi) + ib_2(\xi)], \tag{AI.3}$$

and the complex-valued functions $F_i(\zeta)$ are constructed in Appendix II. It should be pointed out that these functions are well-behaved in the whole range $-\infty < \zeta < +\infty$, with asymptotes

$$F_1(\zeta) = O\left(\frac{1}{\zeta^3}\right), \quad F_2(\zeta) = -\frac{2}{\zeta} + O\left(\frac{1}{\zeta^3}\right) \quad \text{as } \zeta \to \infty. \tag{AI.4}$$

The semi-infinite crack is represented by a distribution of dislocations lying along the negative x_1-axis such that the traction vanishes along the negative x_1-axis. That is, the distribution $B(\xi)$ for $\xi < 0$ must be governed by

$$\int_{-\infty}^{0} \left[\frac{2}{x - \xi} + F_2(x - \xi)\right] \bar{B}(\xi)\,d\xi + \int_{-\infty}^{0} F_1(x - \xi)B(\xi)\,d\xi + 2\pi\beta i\bar{B}(x) = 0,$$

$$\text{for } x < 0, \tag{AI.5}$$

where the first integral is the Cauchy principal value integral. However, (AI.5) is not sufficient to determine $B(\xi)$ unless the asymptotic behaviors at the crack tip and the infinity are specified.

The relative crack face displacements are related to the dislocation distribution by

$$\delta_1(x) + i\delta_2(x) = \int_x^0 [b_1(\xi) + ib_2(\xi)]\,d\xi = \pi i c_2 \frac{1 - \beta^2}{1 + \alpha} \int_x^0 B(\xi)\,d\xi, \quad \text{for } x < 0. \tag{AI.6}$$

The relation between the complex stress intensity factor K and the dislocation distribution B can be derived by combining (2.4) and (AI.6). That is

$$\bar{K} = (2\pi)^{3/2} \sqrt{1 - \beta^2} \lim_{x \to 0} \frac{B(x)}{(-x)^{-1/2 - i\varepsilon}}. \tag{AI.7}$$

The behavior of $B(\xi)$ as $\xi \to -\infty$ can be specified in the way similar to that in the work by Thouless et al. [1]. The results are given below

$$\begin{aligned} \text{Im}\,[B(\xi)] &= -\frac{p^2}{8\pi}[1 + \Sigma\eta(4 + 3\eta) - 6m(1 - \Sigma\eta^2)], \\ & \qquad\qquad\qquad\qquad\qquad\qquad \text{as } \xi \to -\infty, \\ \text{Re}\,[B(\xi)] &= -\frac{p^2}{8\pi}[6\Sigma\eta^2(1 + \eta) + 12m(1 + \Sigma\eta^3)]\xi + \text{real constant}, \end{aligned} \tag{AI.8}$$

where the "real constant" is not known *a priori*. It must be determined as part of the solution to the integral equation. Notice that with asymptotic behaviors (AI.4) and (AI.8), the integrals in (AI.5) are integrable. Since only one loading case needs to be solved, m can be chosen such that Re $[B(\xi)]$ remains finite as $\xi \to -\infty$, i.e.,

$$m = -\frac{6\Sigma\eta^2(1 + \eta)}{12(1 + \Sigma\eta^3)} = -\sqrt{\frac{I}{A}}\sin\gamma. \tag{AI.9}$$

It is believed that (AI.5), (AI.7) and (AI.8) guarantee a unique solution of $B(\xi)$.

Make the change of variables

$$x = \frac{u - 1}{u + 1}, \quad -1 < u < 1, \quad \xi = \frac{t - 1}{t + 1}, \quad -1 < t < 1, \tag{AI.10}$$

and let $\zeta \equiv x - \xi$. Then with $A(t) \equiv B(\xi)$, the integral equation (AI.5) can be reduced to

$$\int_{-1}^{1} \frac{\bar{A}(t)}{u - t}\,dt + \pi\beta i\bar{A}(u) + \int_{-1}^{1} \frac{F_1(\zeta)A(t) + [1 + t + F_2(\zeta)]\bar{A}(t)}{(1 + t)^2}\,dt = 0,$$

$$\text{for } -1 < u < 1, \tag{AI.11}$$

where the first integral is the Cauchy principal value integral. With (AI.7) and (AI.8) in mind, $A(t)$ can be approximated by

$$A(t) = \left(\frac{1 - t}{2}\right)^{-1/2 - i\varepsilon}\left[a_0 + (1 + t)\sum_{k=1}^{N} a_k T_{k-1}(t)\right], \tag{AI.12}$$

where $T_j(t)$ is the Chebyshev polynomial of the first kind of degree j and the a's are complex coefficients which must be determined in the solution process. From (AI.8)

$$\text{Im}\,[a_0] = -\frac{p^2}{8\pi}[1 + \Sigma\eta(4 + 3\eta) - 6m(1 - \Sigma\eta^2)], \tag{AI.13}$$

while the real part of a_0, and the real and imaginary parts of a_k for $k = 1, N$ are unknown.

When substituted into (AI.11), the representation for A leads to an equation of the form

$$\sum_{k=1}^{N}[a_k I_1(u, k) + \bar{a}_k I_2(u, k)] + \text{Re}\,\{a_0\}I_3(u) = I_4(u), \tag{AI.14}$$

where the terms I_j for $j = 1, 4$ involve integrals such as

$$I_1(u, k) = \int_{-1}^{1} F_1(\zeta) T_{k-1}(t)(1 + t)^{-1} \left(\frac{1 - t}{2}\right)^{-1/2 - i\varepsilon} dt. \tag{AI.15}$$

These integrals must be evaluated numerically for given values of u and k.

The solution procedure is as follows. Let a set of $2N$ real unknowns be Re $\{a_0\}$ plus the real and imaginary parts of a_k for $k = 1, N$, excluding the real part of a_N (i.e., effectively, Re $\{a_N\}$ is set to zero). This set of $2N$ unknowns is used to satisfy the real and imaginary parts of (AI.14) at N Gauss–Legendre points $\{u_i\}$ on the interval $-1 < u < 1$. Once the a's have been determined, the complex stress intensity factor can be computed, using (AI.7) and (AI.12), from

$$\bar{K} = (2\pi)^{3/2} \sqrt{1 - \beta^2} \left\{a_0 + 2 \sum_{k=1}^{N} a_k\right\}. \tag{AI.16}$$

The general expression for K in (2.14) applies to the present case with $M = m = -\sqrt{I/A} \sin \gamma$, $P = 1$ and $h = 1$, so that

$$K = \frac{p}{\sqrt{2A}} \cos \gamma \, e^{i\gamma} e^{i\omega}, \tag{AI.17}$$

which yields $\sin \omega$ and $\cos \omega$ independently. The relation $\sin^2\omega + \cos^2\omega = 1$ provides a consistency check on the accuracy of the solution. The results reported in Tables 1–4 were computed with N between 6 and 10. The consistency check was always satisfied to better than 0.3%. It is believed that the accuracy of ω is comparable.

Appendix II

The construction of the dislocation solution used as the kernel in the integral equation (AI.5) is summarized here.

The plane elasticity problem is specified in Fig. 6a. An edge dislocation with components b_1 and b_2 at the origin lies on the interface of two bonded elastic layers. The boundaries of the bi-material layer are traction-free. The problem is solved by superposing the following two solutions.

(i) Two well bonded half-planes with an edge dislocation at the origin (Fig. 6b), and

(ii) Two well bonded layers without edge dislocation (Fig. 6c) but with its upper and lower boundary tractions prescribed as the negative of $\sigma_{22} + i\sigma_{12}$ calculated along $x_2 = h$ and $-H$ in structure (i).

The Muskhelishvili potentials for problem (i) are

$$\Phi(z) = B(1 + \beta^*) \frac{1}{z}, \quad \Psi(z) = \bar{B}(1 - \beta^*) \frac{1}{z}, \tag{AII.1}$$

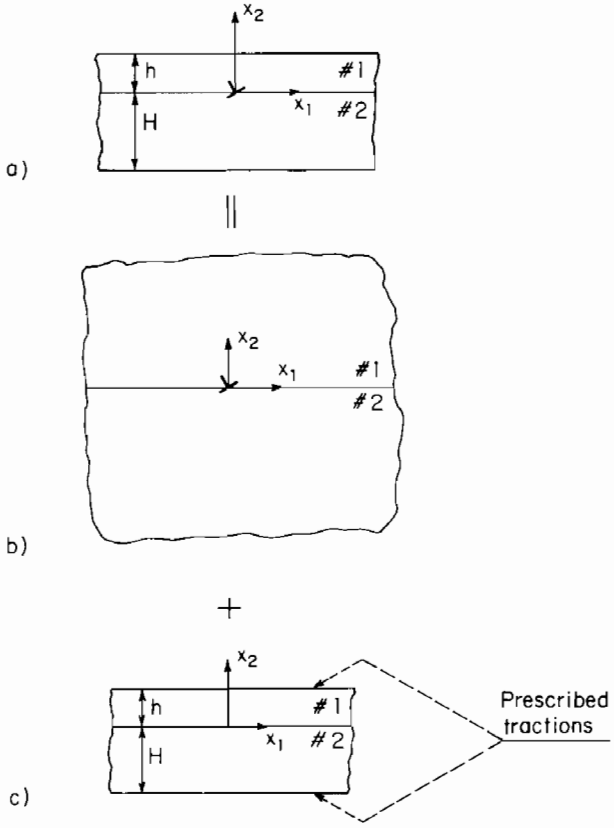

Fig. 6. Conventions for development of kernel function.

where $z = x_1 + ix_2$, $\beta^* = \beta$ for $x_2 > 0$ and $-\beta$ for $x_2 < 0$, and

$$B = \frac{1 + \alpha}{c_2(1 - \beta^2)} \frac{1}{\pi i} (b_1 + ib_2). \tag{AII.2}$$

The stresses calculated from the potentials are given by

$$\sigma_{22}(x_1, x_2) + i\sigma_{12}(x_1, x_2) = \bar{B} \left\{ \left[\frac{2x_1}{r^2} \right] + \mathrm{i} \left[\frac{2\beta^* x_2}{r^2} \right] \right\}$$

$$+ B(1 + \beta^*) \left\{ \left[\frac{4x_1 x_2^2}{r^4} \right] + \mathrm{i} \left[\frac{2x_2}{r^2} - \frac{4x_2^3}{r^4} \right] \right\} \quad \text{for } x_2 \neq 0, \tag{AII.3}$$

and

$$\sigma_{22}(x_1, x_2) + i\sigma_{12}(x_1, x_2) = \bar{B} \left[\frac{2}{x_1} + 2\pi\beta i\delta(x_1) \right] \quad \text{for } x_2 = 0, \tag{A11.4}$$

where $\delta(x)$ is the Dirac delta function and $r^2 = x_1^2 + x_2^2$.

The solution procedure of problem (ii) is similar to that developed in [10] for the homogeneous strip. Only the final results are reported below. The stresses at $x_1 = \zeta$ along the interface of the structure in Fig. 6c are given by

$$\sigma_{22}(\zeta, 0) + i\sigma_{12}(\zeta, 0) = BF_1(\zeta) + \bar{B}F_2(\zeta), \tag{AII.5}$$

where

$$\begin{aligned} F_1(\zeta) &= [Q_2(\zeta) - R_1(\zeta)] + \mathrm{i}[Q_1(\zeta) + R_2(\zeta)], \\ F_2(\zeta) &= [Q_2(\zeta) + R_1(\zeta)] + \mathrm{i}[R_2(\zeta) - Q_1(\zeta)], \end{aligned} \tag{AII.6}$$

where Q's and R's are defined by Fourier integrals

$$\begin{aligned} Q_1(\zeta) &= \int_0^\infty (-C_1 - C_3)\cos\zeta\lambda\,\mathrm{d}\lambda, \quad R_1(\zeta) = \int_0^\infty (-C_1 + C_2 + C_3 + C_4)\sin\zeta\lambda\,\mathrm{d}\lambda, \\ Q_2(\zeta) &= \int_0^\infty (-D_1 - D_3)\sin\zeta\lambda\,\mathrm{d}\lambda, \quad R_2(\zeta) = \int_0^\infty (D_1 - D_2 - D_3 - D_4)\cos\zeta\lambda\,\mathrm{d}\lambda, \end{aligned} \tag{AII.7}$$

where C's and D's are solved from the linear algebraic equations

$$\begin{bmatrix} P_1 \\ P_2 \end{bmatrix} \begin{bmatrix} C_1 D_1 \\ C_2 D_2 \\ C_3 D_3 \\ C_4 D_4 \end{bmatrix} = \begin{bmatrix} X_1 Y_1 \\ X_2 Y_2 \\ X_3 Y_3 \\ X_4 Y_4 \end{bmatrix}, \tag{AII.8}$$

where

$$\begin{aligned} P_1 &= \begin{bmatrix} -\mathrm{e}^{-\lambda h} & -\lambda h\mathrm{e}^{-\lambda h} & -\mathrm{e}^{\lambda h} & -\lambda h\mathrm{e}^{\lambda h} \\ -\mathrm{e}^{-\lambda h} & (1 - \lambda h)\mathrm{e}^{-\lambda h} & \mathrm{e}^{\lambda h} & (1 + \lambda h)\mathrm{e}^{\lambda h} \end{bmatrix} \\ &\quad \times \frac{1}{1 - \alpha} \begin{bmatrix} 1 - \beta & \beta & -(\alpha - \beta) & \beta \\ 0 & 1 + \beta & -2(\alpha - \beta) & -\alpha - \beta \\ -(\alpha - \beta) & -\beta & 1 - \beta & -\beta \\ 2(\alpha - \beta) & -(\alpha - \beta) & 0 & 1 + \beta \end{bmatrix}, \\ P_2 &= \begin{bmatrix} -\mathrm{e}^{\lambda H} & \lambda H\mathrm{e}^{\lambda H} & -\mathrm{e}^{-\lambda H} & \lambda H\mathrm{e}^{-\lambda H} \\ -\mathrm{e}^{\lambda H} & (1 + \lambda H)\mathrm{e}^{\lambda H} & \mathrm{e}^{-\lambda H} & (1 - \lambda H)\mathrm{e}^{-\lambda H} \end{bmatrix} \end{aligned} \tag{AII.9}$$

$$X_1 = -[-\beta - (1 + \beta)\lambda h]e^{-\lambda h},$$

$$X_2 = -[+1 - (1 + \beta)\lambda h]e^{-\lambda h},$$

$$X_3 = -[-\beta + (1 - \beta)\lambda H]e^{-\lambda H},$$

$$X_4 = -[+1 - (1 - \beta)\lambda H]e^{-\lambda H},$$

$$Y_1 = -[+1 + (1 + \beta)\lambda h]e^{-\lambda h},$$

$$Y_2 = +[+\beta - (1 + \beta)\lambda h]e^{-\lambda h},$$

$$Y_3 = -[+1 + (1 - \beta)\lambda H]e^{-\lambda H},$$

$$Y_4 = +[+\beta + (1 - \beta)\lambda H]e^{-\lambda H}.$$

The solution to the problem in Fig. 6a is obtained by superposing (AII.4) and (AII.5), i.e., for the infinite composite strip, the stresses at $(\zeta, 0)$ induced by the dislocation at the origin are given by

$$\sigma_{22}(\zeta, 0) + i\sigma_{12}(\zeta, 0) = \bar{B}\left[\frac{2}{\zeta} + 2\pi\beta i\delta(\zeta) + F_2(\zeta)\right] + BF_1(\zeta). \tag{AII.10}$$

Appendix III

The superposition scheme in Figs. 1a–c is outlined here. The neutral axis of the composite layers in Figs. 1a and b is a distance δ above the bottom of layer #2, where δ is given by

$$\frac{\delta}{h} \equiv \Delta = \frac{1 + 2\Sigma\eta + \Sigma\eta^2}{2\eta(1 + \Sigma\eta)}. \tag{AIII.1}$$

The stresses in the composite beam in Fig. 1b are $\sigma_{22} = \sigma_{12} = 0$ and

$$\sigma_{11}(y) = \begin{cases} \Sigma\left(\dfrac{P_3}{hA_0} + \dfrac{M_3}{h^3 I_0}\, y\right), & H - \delta < y < H - \delta + h \\ \dfrac{P_3}{hA_0} + \dfrac{M_3}{h^3 I_0}\, y, & -\delta < y < H - \delta, \end{cases} \tag{AIII.2}$$

where y is measured from the neutral axis and

$$A_0 = \frac{1}{\eta} + \Sigma,$$

$$I_0 = \frac{1}{3}\left\{\Sigma\left[3\left(\Delta - \frac{1}{\eta}\right)^2 - 3\left(\Delta - \frac{1}{\eta}\right) + 1\right] + 3\,\frac{\Delta}{\eta}\left(\Delta - \frac{1}{\eta}\right) + \frac{1}{\eta^3}\right\}. \tag{AIII.3}$$

The equivalent loads P and M in Fig. 1c are obtained by superposing the structures in Figs. 1a and b. That is

$$P = P_1 - \int_{H-\delta}^{H-\delta+h} \sigma_{11}(y)\,dy,$$
$$M = M_1 - \int_{H-\delta}^{H-\delta+h} \sigma_{11}(y)\left[y - \left(H - \delta + \frac{h}{2}\right)\right] dy. \tag{AIII.4}$$

Substitution of (AIII.2) into (AIII.4) gives

$$P = P_1 - C_1 P_3 - C_2 \frac{M_3}{h}, \quad M = M_1 - C_3 M_3, \tag{AIII.5}$$

where

$$C_1 = \frac{\Sigma}{A_0}, \quad C_2 = \frac{\Sigma}{I_0}\left(\frac{1}{\eta} - \Delta + \frac{1}{2}\right), \quad C_3 = \frac{\Sigma}{12 I_0}. \tag{AIII.6}$$

Notice that C's depend on η and Σ only.

References

1. M.D. Thouless, A.G. Evans, M.F. Ashby and J.W. Hutchinson, *Acta Metallurgica* 35 (1987) 1333–1341.
2. M.S. Hu, M.D. Thouless and A.G. Evans, *Acta Metallurgica* 36 (1988) 1301–1307.
3. M.D. Drory, M.D. Thouless and A.G. Evans, *Acta Metallurgica* 36 (1988) 2019–2028.
4. Z. Suo and J.W. Hutchinson, Steady-state Cracking in Brittle Substrates beneath Adherent Films, Harvard University Report MECH-132 (1988), to appear in *International Journal of Solids and Structures*.
5. P.G. Charalambides, J. Lund, A.G. Evans and R.M. McMeeking, *Journal of Applied Mechanics* 56 (1989) 77–82.
6. J.R. Rice, *Journal of Applied Mechanics* 55 (1988) 98–103.
7. J. Dundurs, in *Mathematical Theory of Dislocations*, American Society of Mechanical Engineering, New York (1969) 70–115.
8. J.W. Hutchinson, M.E. Mear and J.R. Rice, *Journal of Applied Mechanics* 54 (1987) 828–832.
9. G.P. Cherepanov, *Mechanics of Brittle Fracture*, Chapter 9, McGraw-Hill, New York (1979).
10. M.B. Civelek, in *Fracture Mechanics: Sixteenth Symposium*, STP 868, M.F. Kanninen and A.T. Hopper (eds.), American Society for Testing and Materials, Philadelphia (1985) 7–26.
11. M.Y. He and J.W. Hutchinson, Kinking of a Crack Out of an Interface, Harvard University Report MECH-113 (1988), to appear in *Journal of Applied Mechanics*.

Résumé. On considère une fissure d'interface semi-infinie entre deux couches infinies élastiques et isotropes soumises à des conditions générales de sollicitations sur leurs bords. Le problème peut être solutionné par voie analytique, à l'exception d'un scalaire réel simple, indépendant de la charge, qui est extrait de la solution numérique relative à une combinaison particulière des sollicitations.

On procède à deux applications de la solution de base qui illustrent son utilité: l'une est relative à une fissure d'interface soumise aux tensions résiduelles dans un film mince déposé sur un substrat. L'autre est l'analyse d'une éprouvette d'essai proposée récemment pour mesurer la ténacité de l'interface.